

Lidar observations of sodium layer over low latitude, Gadanki (13.5° N, 79.2° E): seasonal and nocturnal variations

P. Vishnu Prasanth¹, V. Sivakumar^{1,2,3}, S. Sridharan⁴, Y. Bhavani Kumar⁴, H. Bencherif¹, and D. Narayana Rao⁵

¹Laboratoire de l'Atmosphère et des Cyclones (LACy), UMR 8105, CNRS, Université de La Réunion, Reunion Island, France

²National Laser Centre (NLC), Council for Scientific and Industrial Research (CSIR), P.O. Box 395, Pretoria 0001, South Africa

³Department of Geography, Geoinformatics and Meteorology, University of Pretoria, Lynwood Road, Pretoria 0002, South Africa

⁴National Atmospheric Research Laboratory, Department of Space, Gadanki, India

⁵SRM University, Kattankulathur, India

Received: 5 February 2009 – Revised: 25 September 2009 – Accepted: 29 September 2009 – Published: 7 October 2009

Abstract. In this paper, we present seasonal and nocturnal variations of mesospheric sodium (Na) layer parameters observed over Gadanki (13.5° N, 79.2° E), based on 166 nights during the period from January 2005 to December 2006, for the first time. The total Na content decreases during the evening and reaches a minimum value around midnight and maximum in the early morning. The year-to-year variations illustrate that Na layers reach the peak value close to 93.5 km for the year 2005 and ~93 km for the year 2006 and falls to near zero value around 110 km. Though, seasonal variation of sodium density illustrate maximum values in September, December and March, we require a larger data base for September months to conclude the statement. The column abundance shows maximum during autumn equinox and minimum during winter. The obtained seasonal and nocturnal variation of sodium layer parameters are compared with mid-latitude observations and further possible mechanisms are discussed.

Keywords. Atmospheric composition and structure (Middle atmosphere – composition and chemistry) – Meteorology and atmospheric dynamics (Middle atmosphere dynamics; Waves and tides)

1 Introduction

Meteoric ablation is the source of the layer of neutral sodium (Na) atoms that occurs globally in the Mesosphere and Lower Thermosphere (MLT) region (Plane, 2003). The Na layer was discovered nearly 80 years ago: radiation at 589 nm was observed in the night sky spectrum (Slipher, 1929). The mesospheric Na, owing to its large resonant backscatter cross section and relatively high column abundance, has been widely used to study the middle atmospheric dynamics and chemistry.

Large evidences of Na observations were made over the globe using ground based lidars (Bowman et al., 1969; Gibson and Sandford, 1971; Gibson and Sandford, 1972; Megie and Blamont, 1977; Clemesha et al., 1979, 2004; Kirchoff and Clemesha, 1983; Gardner et al., 1988; Tilgner and von Zahn, 1988; von Zahn et al., 1988; Plane et al., 1999; She et al., 2000; Gardner et al., 2005; Bhavani kumar et al., 2007b), satellite borne (Newman, 1988; Fussen et al., 2004; Gumbel et al., 2007; Fan et al., 2007), and other instruments (Slipher, 1929; Hunten, 1954; Chamberlain, 1956; Hunten and Wallace, 1967). The first satellite-borne observations of sodium nightglow were made by Newman (1988) but Clemesha et al. (1990) argued the accuracy of the measurements for very low equatorial profiles. Fussen et al. (2004) reported global measurements of the mesospheric Na layer by using the GOMOS (Global Ozone Monitoring by Occultation of Stars) stellar occultation instrument onboard of ENVISAT (Environment Satellite) satellite. But, the retrieved Na column abundances, layer density profiles, seasonal and latitudinal variations were found to be in poor agreement with the



Correspondence to: P. Vishnu Prasanth
(vishnuprasanthp@gmail.com)

available data from ground-based lidars (Fan et al., 2007). Gumbel et al. (2007) developed a new method using optimal estimation theory (Rodgers, 2000) to retrieve the absolute mesospheric Na density profiles from limb-scanning satellite observations of the Na D-lines based on the day glow techniques. This method has been validated by comparing Na profiles retrieved from the OSIRIS (Optical Spectrograph and Infrared Imager System) spectrometer on the Odin satellite, and Na lidar at Ft. Collins, Colorado. Their retrieved column abundance and density profiles are found to be in good agreement with mid-latitude lidar observations (Gardner et al., 1986). Earlier results from the researchers reported that the Na layer exhibits seasonal variations at all latitudes higher than 20° (Simonich et al., 1979; Gardner et al., 1986; Gibson and Sandford, 1971; Fan et al., 2007), the Na layer column density minimum near the summer solstice and maximum during early winter. But, few measurements at low-latitudes observed the less seasonal variation in the Na layer (e.g. Fan et al., 2007).

Over few decades, numerous chemical and dynamical processes have been proposed with an attempt to explain the general characteristics of seasonal, diurnal, and geographical variations of the Na layer structure. The seasonal and geographical variations in Na abundance at mid- and low-latitudes are now believed to be related to changes in the mesopause temperature that affect the reaction rates of the main chemical loss processes for Na (see Gardner et al., 1986). Much of the intrinsic character of the layer is apparently governed by a complex chemistry involving many reactions among numerous neutral and ionic species (Sze et al., 1982; Kirchoff, 1983; Jegou et al., 1985a). The dominant loss mechanisms are believed to include the conversion of neutral sodium into NaO₂ through a reaction with O₂ and any other molecules or atoms (N₂ and H₂) (Swider, 1985) and the formation of cluster ions followed by the formation of particles which then precipitate to the lower atmosphere (Richter and Sechrist, 1979a, b; Jegou et al., 1985a). These two reactions are particularly interesting because of their temperature dependence based on the heating rate coefficients that may explain seasonal and geographical variations in the sodium abundance (Swider, 1985; Jegou et al., 1985a, b). The further conversion of NaO₂ to NaOH may also be an important component of the loss processes (Kirchhoff and Clemesha, 1983; Kirchhoff, 1983). In addition to chemical activity, the dynamic effects of tides, gravity waves and turbulence have shown a significant influence on the vertical structure of the layer (Rowlett et al., 1978; Richter et al., 1981; Batista et al., 1985). However, the summertime depletion of Na above Andoya (69° N) (von Zahn et al., 1988) and Spitsbergen (78° N) (Gardner et al., 1988) in the Norwegian Arctic suggests that other loss mechanisms, such as Na absorption by polar mesospheric cloud particles, absorption on smoke, dust particles and photo-ionization may be very important at high latitudes.

Detailed information about the mesospheric atomic sodium layer has been gathered using lidar measurements

around the globe. Gibson and Sandford (1971) at Winkfield, England (51° N, 1° W) made the first lidar observations on seasonal variations of the sodium layer. They found that the seasonal variation of the layer shows that the winter maximum of abundance due to increase of bottom-side of the Na layer and summer minimum in abundance is caused by a loss of Na from the topside. Later on, many similar measurements have also been reported (Megie and Blamont, 1977; Simonich et al., 1979; Gardner et al., 1986; States and Gardner, 1999; Plane et al., 1999; She et al., 2000).

Megie (1976) showed negligible nocturnal variation in sodium density on the bottom side of the layer. Simonich et al. (1979) observed that the average nocturnal variation is consistent with photochemical control over bottom side of the layer and diffusive control on topside. Variations observed on individual nights appear to be mainly dynamic in origin. Gardner et al. (1986) also observed the nocturnal variations of sodium layer parameters and structure. The diurnal variations of Na abundance and densities above 90 km are controlled by photo ionization and charge exchange reactions during the day and recombination during night (States and Gardner, 1999). However, the measurements in the tropical region are very few in comparison to those available at mid- and high- latitudes. Over tropics, the observations were made only at Mauna Kea, Hawaii (20° N) (Kwon et al., 1988) and Arecibo, Puerto Rico (18° N) (Beatty et al., 1989) except few measurements are available at lower latitudes (Clemesha et al., 1998; Fan et al., 2007). In addition, the obtained results are based on few days of measurements and there is no systematic study on seasonal variation of the Na layer at these latitudes. Further, the report by Clemesha et al. (1998) observed that the occurrence rate of sporadic Na layers at a Southern Hemisphere low latitude site was quite different compared to the Northern Hemisphere low latitude location (see also Kwon et al., 1988). Thereby, the measurements of mesospheric sodium at least probed low latitude sites are important and it is valuable to understand the nocturnal, seasonal and latitudinal behavior and dynamics of atmospheric sodium layer. Moreover, the study helps researchers to develop or add an input to the global models.

In the present study, we describe the first results of the seasonal and nocturnal variations of mesospheric Na layer as derived from lidar over a low latitude site, Gadanki, for the period from January 2005 to December 2006. The study is also motivated by the earlier report from Gadanki that the occurrence rate of sporadic Na layers is higher than the one at other stations (Vishnu Prasanth et al., 2007). The present paper is organized as follows; the resonance lidar system setup and data analysis are described in Sect. 2. The general characteristics of sodium layer, such as its vertical distributions, temporal variations in terms of nocturnal, day-to-day, seasonal variations, and mean characteristics of column abundance, centroid, RMS width, and its altitude variations, are described in Sect. 3. Summary of the obtained results are presented in Sect. 4.

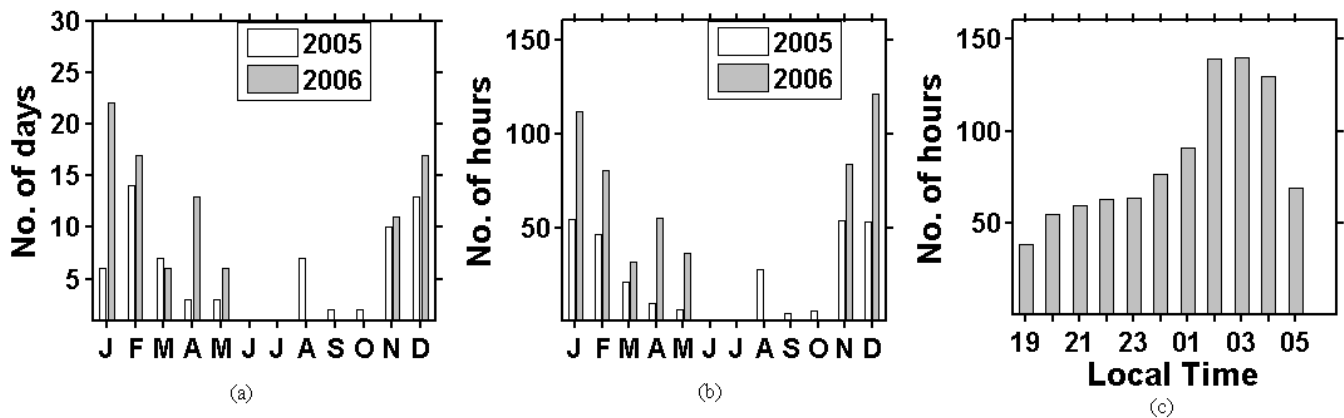


Fig. 1. Histograms showing monthly distribution of data for the period from January 2005 to December 2006 (a) number of days, (b) number of hours of sodium lidar data and (c) number of observational hours per local time.

2 Resonance lidar set-up and data analysis

A state-of-the-art Rayleigh and Mie backscattering lidar set-up was established at a low latitude station, Gadanki (13.5° N, 79.2° E) under Indo-Japanese collaboration programme in 1998 (Bhavanikumar et al., 2000). Recently, the lidar system capability was augmented for measuring the mesospheric sodium. The power-aperture product of the lidar system is ~ 0.35 W m². The transmitter consists of a tunable pulsed dye laser pumped by a frequency-doubled Nd:YAG laser. The pulsed dye laser is tuned to the D_2 resonant absorption line of Na at a wavelength near 589 nm. The dye laser employs a dual grating system that is controlled by a computer which enables a rapid selection of transmitted wavelength. The line width of laser is about 2 p.m. The dye laser is pumped with 200 mJ at 532 nm to get output pulse energy of 25 mJ at 589 nm. The dye laser uses Kiton-Red medium and the end shape of laser beam is rectangular with beam divergence less than 0.5 mrad. The receiving system uses a 750 mm Newtonian telescope with field optics and an interference filter. We employed photomultiplier tube (PMT) for detecting the backscattered photons. The output pulses of the PMT are amplified by a broadband amplifier and then fed into a PC based photon counting multi channel scalar (MCS). The MCS counts the pulses in successive time bins. Each time bin is set to 2μ s, corresponding to a vertical resolution of 300 m. The photon counts are accumulated for 2400 shots which correspond to a time-resolution of 120 s. The sodium concentration profiles are derived directly from the photon counts. The system details and the method of estimation of sodium concentration profiles were described in Bhavanikumar et al. (2007a).

The lidar system has been operated for sodium layer observations from January 2005 and has produced significant amount of data. The sodium lidar data used in this study are collected over 166 nights during the period from January 2005 to December 2006. Observations were made at a time-

and height- resolutions of 120 s and 300 m, respectively, and usually for the duration of three to eleven hours limited to nocturnal periods. On some occasions, the observations are necessarily restricted to shorter periods due to unfavourable atmospheric background conditions, such as convective and cloudy conditions (June, July) over the site (Kumar and Jain, 2006). The number of observational days per month and number of hours per month used in the present study for the period from January 2005 to December 2006 are shown in Fig. 1a and b. It is noted that there are more observations during 2006 in comparison to 2005, as more experiments were planned specifically for sodium layer during 2006. During few months (June–July 2005 and June–October 2006), the lidar observations were not possible due to background atmospheric conditions and partly due to system technical problems. The total number of hours of observations for the above said period is presented in histogram (see Fig. 1c). It is evident from the figure that at least each hour accounted for minimum number of ~ 40 observations (hourly slots) which would be sufficient to reveal any temporal (nocturnal) characteristics of the observed sodium layer.

3 Results and discussion

3.1 General characteristics of the sodium layer: spatial distribution

Figure 2 shows a series of height profiles of sodium layer averaged over different time intervals. The profiles illustrate the mean structure for 2 min, 1 h, over night (6 h) for 10 January 2005 and two consecutive nights along with 11 January 2005. As mentioned earlier in the previous section, each individual profile corresponds to 2400 laser shots (~ 2 min). The first profile in the figure is averaged over 2 min and the corresponding measurement error is shown in the figure (vertical bar) which is proportional to the square root of the photon

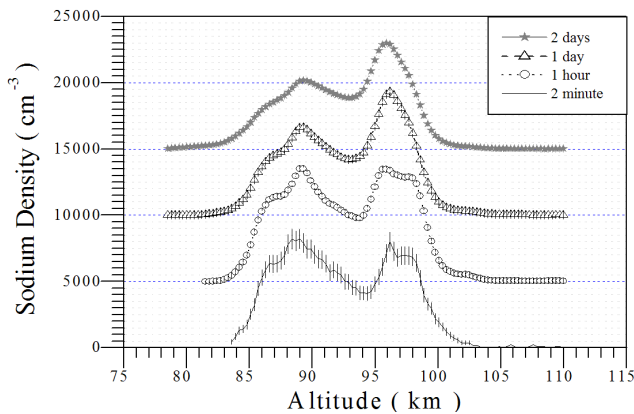


Fig. 2. Height profile of sodium density averaged over different time scales. The vertical bar represents the statistical error in the retrieved Na concentration. The profiles are vertically offset by 5×10^3 .

count at each height. For 2-min profile, the statistical error values in the measured density at ~ 92 km reaches upto 10%. As expected statistically, the measurement error decreases by increasing the temporal integration for 1 h ($\sim 2\%$), 1 day ($\sim 1\%$) and 2 days (0.5%). It is noted here that there is an invisible error bar (more than 2 min) which is due to the artifact of scaling. It is basically due to the fact that the error bar is much less than the actual measurements. The 2-min profile shows a structure with two distinct peaks. An average of thirty profiles correspond to 1 h observations of the same night between 00:30 and 01:30 LT also show the similar double-peak structure. Such double-peak structure is usually observed in our data while averaged over short time periods. In some events, even three peaks are maintained for several hours. The observed double-peak structure is in accordance with the results obtained by Sandford and Gibson (1970) in England, by Blamont et al. (1972) in France, and by Simonich et al. (1979) in Brazil. The mean profile obtained for complete night observations (~ 6 h) also shows two distinct peaks, which is very occasionally observed for such longer periods of time. An average over two nights for 10 and 11 January 2005 shows almost similar structure as observed for the previous night (10 January 2005). The period of observations used in the two nights is about 15 h. In general, all the profiles display primary and secondary peaks at 97 km and 87 km, respectively. It is observable from the figure that the primary peak becomes broader and the secondary peak becomes narrower when averaging over longer time intervals. Individual profiles, which usually represent a time average of 2 min, show a considerable amount of fine structures, which disappear when time integration is longer. Moreover, the plateau type of structure is observed more frequently. These fluctuations might be caused either by short-scale wave disturbances or by the horizontal movement of spatial irregularities in the layer (Simonich et al., 1979). An illustrative

example is discussed in Sect. 3.3 for a typical case. The existence of horizontal structure in the mesosphere was also reported from OH nightglow observations (Krassovsky, 1977). A more detailed night-to-night variation is discussed in the following section (see Sect. 3.2).

3.2 Temporal (night-to-night) variations

We have considered a continuous 12 night observations from 5 to 16 February 2005 to understand the night-to-night variability in the mean sodium layer structure. Figure 3a represents the contour plot of sodium layer density and the corresponding mean structures of its abundance, centroid and RMS (Root Mean Square) width are plotted in Fig. 3b. The contour plots are based on height profiles averaged over 4 h from 01:00 LT to 05:00 LT. It is clearly seen from the Fig. 3a that the distribution shows appreciable continuity over a period of several nights, although significant changes sometimes occur from one night to another, as in the case of 12 February, which is accompanied by a major change in the vertical distribution of sodium. This particular day is an exceptional day when the Na density over Gadanki enhanced to the greatest amount ever been observed value of $60\,722$ atoms/cm³ at 92 km (Vishnu Prasanth et al., 2007). The maximum Na density peak over Gadanki is 2.5 times more than that of mid- and high-latitudes (Fan et al., 2002; von Zahn et al., 1987). It may be mentioned here that the atmospheric waves may also cause such distortions on the mean sodium layer structure (Gardner and Voelz, 1987; Clemesha et al., 2001).

3.3 Atmospheric wave influences on the sodium layer

Figure 4 shows a contour plot of sodium density layer for the night of 15/16 January 2006 and the abundance curve (overlapped solid line in the figure) for the same day. These profiles were obtained during the time interval 18:50–05:00 LT on 15/16 January 2006. The maximum and minimum column abundances over this particular night are $\sim 2.01 \times 10^{10}$ atoms/cm² and $\sim 6.98 \times 10^9$ atoms/cm², respectively observed at 20:39 LT and 03:31 LT. The predominant feature seen in this plot is the peak height decrease throughout the night. The descending structure represents perturbation due to atmospheric wave propagation. In general, we find a descending structure in the sodium layer in the height region between 94 and 98 km in most of our observations. Simonich et al. (1979) also observed the decrease in the height of peak density throughout the night over southern sub-tropics (Brazil).

The nocturnal variations of the sodium layer structure are usually dominated by atmosphere wave dynamics. In general, planetary waves, tides and gravity waves, which originate from the troposphere, propagate up to the mesosphere height regions and dissipate their energy near the mesopause making important contributions to the momentum and

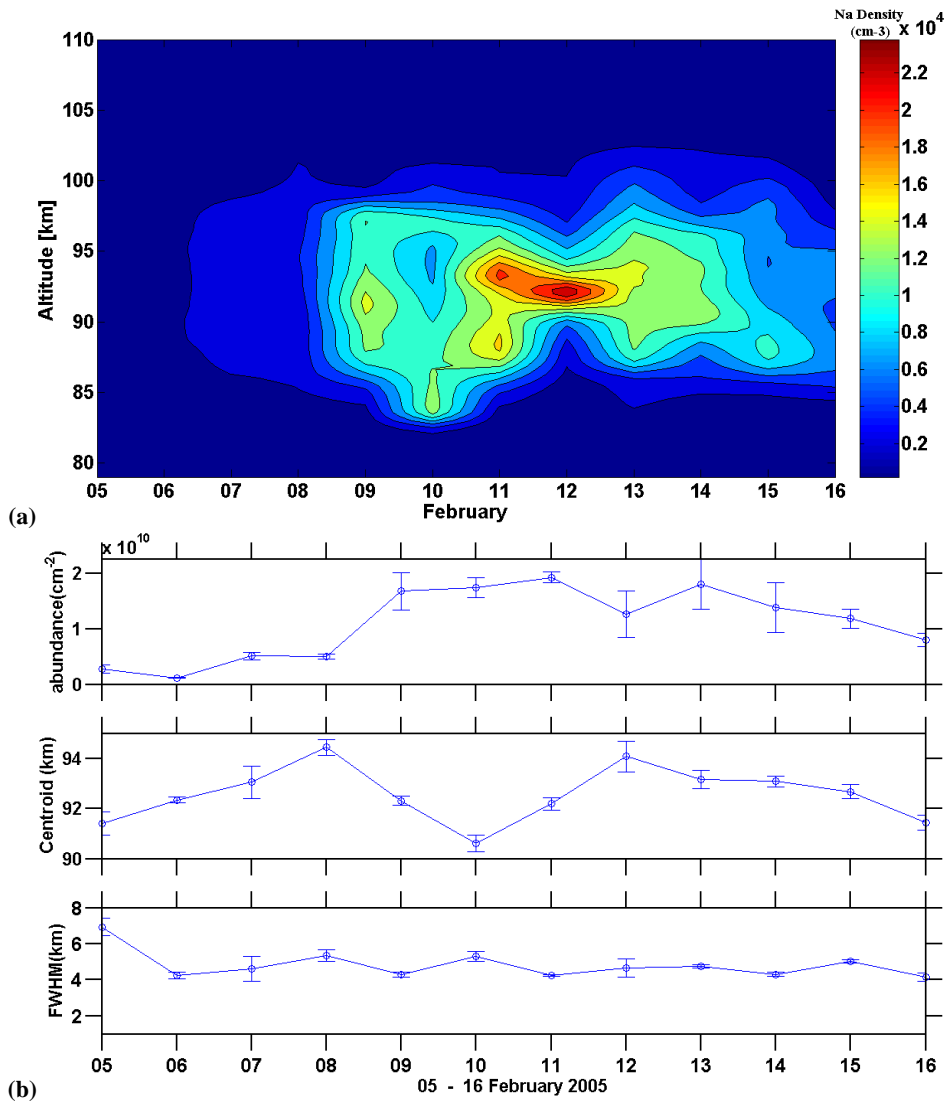


Fig. 3. (a) Contour plots of the averaged Na density (cm^{-3}) for the period from 5–16 February 2005. (b) Day-to-day variations of Na abundance, centroid and RMS width obtained during the above said period (5–16 February 2005) over Gadanki by lidar.

turbulence budget in this region of the atmosphere (Gardner et al., 1986). The propagating wave induced features in the layer are virtually apparent in all the observations made at Gadanki. These features include propagating stratifications in the density profiles (Gardner and Voelz, 1985) and perturbations in the abundance, centroid height and RMS width parameters (Gardner and Shelton, 1985). To illustrate the wave distortions in the sodium layer, we present a typical observation in this section.

Figure 5a illustrates how the wave dynamic influence the above mentioned sodium layer parameters on 2 April 2006. The small variations in these parameters observed before midnight are typical of gravity wave induced perturbations (Gardner et al., 1986; Gardner and Shelton, 1985). At 19:30LT the column abundance reaches a maximum

value of $1.48 \times 10^{10} \text{ cm}^{-2}$ and then rapidly decreases reaching a value of $6.89 \times 10^9 \text{ cm}^{-2}$ at about 21:03LT. The centroid and RMS width also begins to oscillate with respect to the column abundance in the time interval 19:30LT to $\sim 02:30$ LT. The peak-to-peak amplitudes of the abundance, centroid height and width oscillations are approximately $7.9 \times 10^9 \text{ cm}^{-2}$ (215%), 1.64 km and 0.9 km, respectively. The width and centroid oscillations are in phase but as expected out of phase with the abundance oscillations. The centroid generally decreases due to the increase in sodium occurs on the bottom side of the layer (Gardner et al., 1986). This is illustrated in Fig. 5b where the measured 15-min sodium profiles are plotted on a linear scale. Enhancements of the sodium content at 87 km are clearly evident near 19:30LT, the time when the abundance reaches local

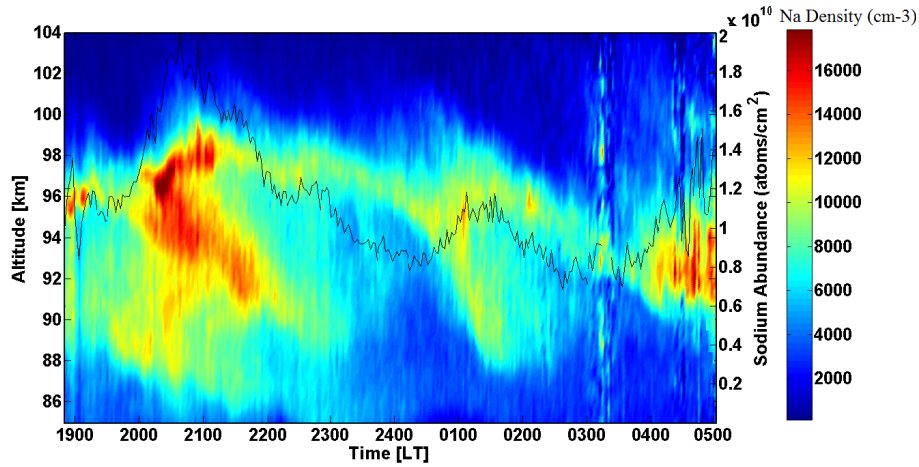


Fig. 4. Contour plot of sodium density layer observed for the night of 15/16 January 2006 and the abundance (solid line) for the same day in the figure.

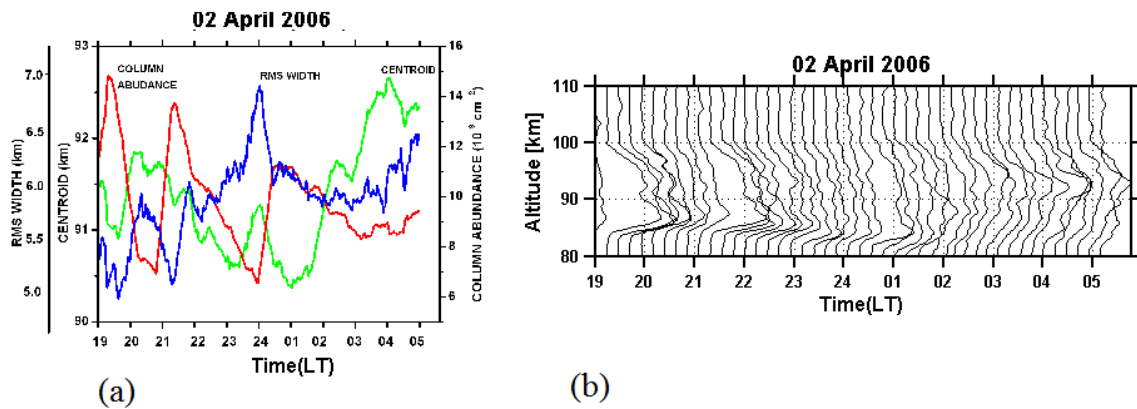


Fig. 5. Temporal variations of the sodium layer column abundance (red line), centroid height (green line) and RMS width (blue line) measured on the night 2/3 April 2006 are shown in (a). Height profiles of sodium density are plotted in panel (b), where the profiles are plotted on a linear scale at 15-min intervals.

maxima, and the centroid and width are minimum. There are indications that dense clouds can be formed by excess sodium deposition due to meteoric ablation (Kirchhoff and Takahashi, 1984; Gardner et al., 1986). However, the oscillations in Fig. 5b suggest a wave-like horizontal stratification which may have been caused by the interaction of wave motions with the background wind profile (Gardner et al., 1986).

3.4 Seasonal variations

3.4.1 Seasonal variations of sodium density

Figure 6 shows the height-month contour plot of sodium density obtained from the two-year datasets (January 2005 to December 2006). The data has been grouped in terms of month, irrespective of the years and used for calculating the mean. The number of Na profiles used for each month and the corresponding year are given in Fig. 1 (see

Histogram). It should be noted here that during 2005 and 2006, there were no data available for June and July months. In addition to this, there are no lidar observations from August to October 2006, thereby; we have used only the year 2005 data for those corresponding months. Due to the lack of data in June and July for 2005 and 2006, we have plotted Fig. 6 from August to May. Figure 6 illustrates a clear seasonal variation in sodium density over height and by its structure. The sodium density peaks in September, December and March. However, the peak observed during September needs to be confirmed using larger datasets. It is clearly noticed that the sodium density during March and December is smaller in magnitude than that observed in September. Fan et al. (2007) observed that the maximum Na layer density usually occurs in October–November in the Northern Hemisphere and from May to August in the Southern Hemisphere. It is in quite agreement with the maximum density

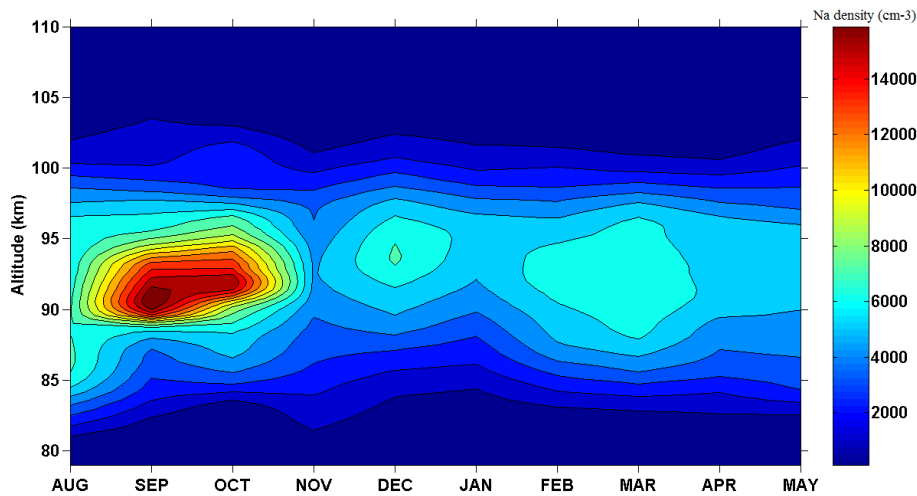


Fig. 6. Height-month contour plot of average seasonal variation of sodium density (cm^{-3}) obtained from lidar observations in 2005–2006 over Gadanki.

observed at Gadanki during September and also the results reported for mid-latitude using lidar (States and Gardner, 1999). However, more LIDAR data from our site is required (especially for September) to conclude the statement. The causative mechanisms which contribute to such maximum is not yet fully understood. The maximum sodium density occurrence in all the months is approximately between 90 and 95 km, added to it, Gadanki observations show a broad maximum from August to November from 84 km to 96 km. She et al. (2000) observed that the maximum and minimum mean peak sodium densities were $4.88 \times 10^9 \text{ m}^{-3}$ at 91 km and $1.49 \times 10^9 \text{ m}^{-3}$ at 90 km occurring in November and June, respectively. Gibson and Sandford (1971), at Winkfield England (51° N) and Megie and Blamont (1977), at Haute-Provence France (44° N), found that the winter maximum is confined to only for a few months (~ 2 month), while the rest of the year is characterized with relatively small density variations. At high latitudes, the seasonal variations in density layer vary from summer minimum to winter maximum (Fan et al., 2007). Simonich et al. (1979) at 23° S observed a broad maximum from early autumn to late spring. The winter maximum in density is observed at the northern mid-latitudes appears to result from a large increase in sodium density on the bottom side of the layer.

Na^+ ions and sodium bicarbonate (NaHCO_3) are the major reservoir species above and below the atomic Na layer, respectively (Plane et al., 1999; Plane, 2004). Due to long residence time (~ 7 days) of ablated sodium in the region between 80 and 100 km (Plane, 2004) and the comparatively short lifetimes of the rate-determining chemical reactions that convert sodium between atomic Na and these reservoirs, the chemistry reaches a photochemical steady-state on the timescale of vertical transport by eddy or molecular diffusion (Plane et al., 1998). Therefore, atmospheric chemistry plays a key role in determining the atomic Na distribution.

3.4.2 Seasonal variations of sodium layer parameters

Column abundance

Figure 7a shows seasonal variation of sodium layer column abundance for the years 2005 and 2006 at Gadanki. As it can be seen from Fig. 1a, during 2006, the lidar was not operational for 5 consecutive months, i.e., from June to October. Indeed, the August, September, and October monthly mean sodium profiles are derived only from 2005 lidar observations. Due to prevailing monsoon conditions (June and July) and few lidar technical problems (August 2006, September 2006 and October 2006), the measurements were not possible. Due to the lack of data in June and July, we plotted from August to May in Fig. 7a, b, c. During 2005, the column abundance value shows a maximum during September with a value of $1.37 \times 10^{10} \text{ cm}^{-2}$ and a minimum of $4.55 \times 10^9 \text{ cm}^{-2}$ during January. Our observations illustrate a maximum in abundance during autumn equinox and minimum in the winter months. These observations are in contrast with other Northern and Southern Hemisphere lidar measurements (Gibson and Sandford, 1971; Megie and Blamont, 1977; Gardner et al., 1986; Simonich et al., 1979), who reported maximum during winter and summer minimum. Gardner et al. (1986) observed a sharp winter maximum and broader summer minimum and Megie and Blamont (1977) observed a winter maximum and broad minimum abundance throughout the summer months. From Gadanki observations, the maximum abundance measured during September is approximately 3 times greater than the January minimum value. However, we require a larger data base to conclude our statements. The measured column abundance values are consistent with the results of Megie and Blamont (1977) and Gardner et al. (1986).

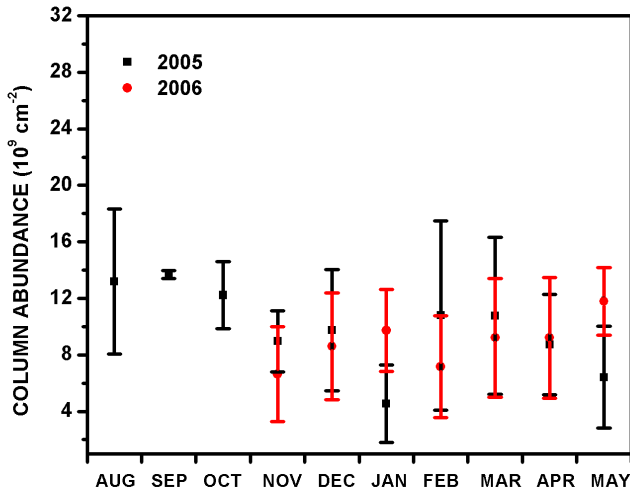


Fig. 7a. Monthly mean Sodium layer column abundance obtained during the years 2005 and 2006.

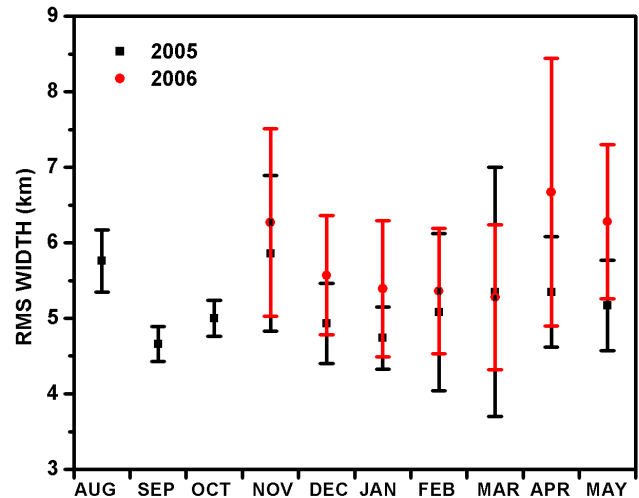


Fig. 7c. Same as Fig. 7a, but for RMS width.

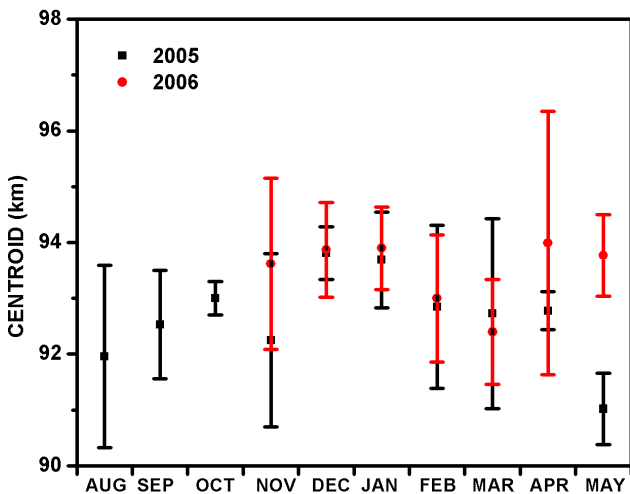


Fig. 7b. Same as Fig. 7a, but for Centroid height.

Centroid

Figure 7b shows the seasonal variation of the centroid height obtained from the years 2005 and 2006 over Gadanki. The layer centroid height has an average value of 93 km which is comparable to the values reported from mid-latitude station by Gardner et al. (1986). The seasonal variation of the centroid height does not reveal any significance (based on obtained the standard deviations); it might be due to insufficient statistic. Gardner et al. (1986) mentioned that the SAO in the centroid height with maximum during March and September. They have suggested that such oscillation might be due to the meridional mesospheric circulation system. Gibson and Sandford (1971) at 51° N found that the peak of the layer decreased substantially from about 92 km in summer to about 87.5 km in November-December and January. The lower-

ing of the peak was associated with a significant increase in sodium on the bottom side of the layer (Gardner et al., 1986). Megie and Blamont (1977) at 44° N also found a decrease in the apparent layer peak from approximately 91 km in summer to about 89 km in late winter. However, over southern sub-tropics, Simonich et al. (1979) did not find any significant seasonal variations in the height or structure of the layer.

RMS width

Figure 7c shows seasonal variation of the RMS width of the sodium layer obtained from the two years period over Gadanki. The RMS width has a primary maximum in April and a secondary maximum during November. The RMS width is larger in 2006 in all the months compared to the 2005 RMS width. The average RMS width over Gadanki is approximately ~5.5 km. This value is 20% more than the report available for low-, mid- and high-latitudes (Beatty et al., 1992; Gardner et al., 1986; Collins et al., 1994). Gardner et al. (1986) observed no significant seasonal variation of the RMS layer width while the average RMS width was found to be ~4.25 km. States and Gardner (1999) reported seasonal variations in the RMS width of the Na layer that are smaller than at high latitudes.

3.5 Mean nocturnal variations of the sodium layer

The mean nocturnal variation of the sodium layer is obtained based on the two years of data and is plotted in Fig. 8. In the data collected from January 2005 to December 2006, we have ~40 days of sodium density observations for the entire time period from 19:00 to 06:00 LT. Hence, we restricted the analysis on nocturnal variation of the sodium layer to these 40 days only, which ensures homogeneity of the used dataset. It is noted that the above mentioned ~40 days observations are mostly during winter months (see Fig. 1). In this figure,

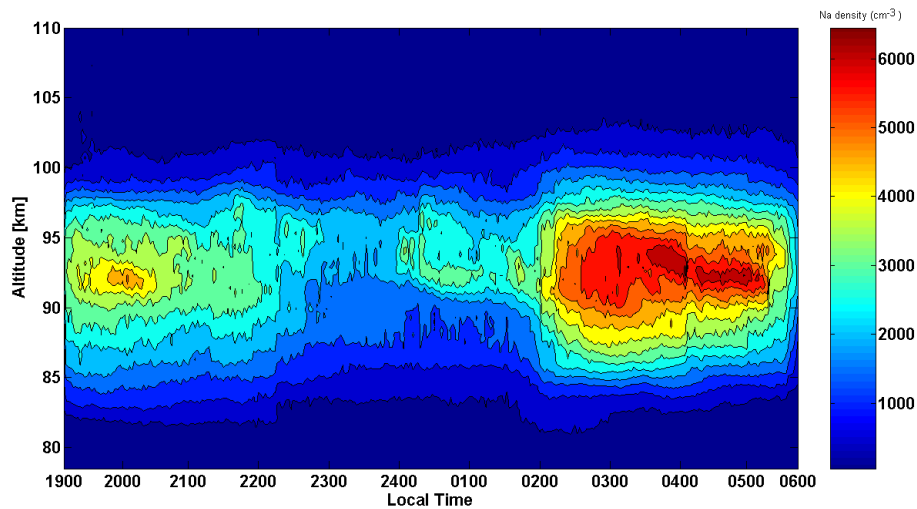


Fig. 8. Mean Nocturnal evolution of mesospheric sodium layer as obtained from lidar observations in 2005 and 2006.

we have considered the temporal variations from 19:00 to 06:00 LT, even though we had the data before 19:00 h and after 06:00 h when the frequency of observations is very few (less than or equal to 3). The most prominent features of the density contour plot in Fig. 8 are the two maxima found at 92.6 km around 04:04 LT and 92 km around 20:08 LT. Moreover, there is an increase of sodium above 95 km. Takahashi et al. (1977) reported that the average nocturnal variations showed maximum intensities just after 03:00 LT. Simonich et al. (1979) also found that the maximum Na density occurred around 03:00 LT. Gardner et al. (1986) observed the peak of the layer reaching a maximum density of about 5500 cm^{-3} near 03:00 LT. They also noted increase of sodium above 95 km and a decrease below 80 km during the night. States and Gardner (1999) have shown that the maximum density at the peak layer of 3630 cm^{-3} at 91.8 km at 04:40 LT.

Further, the structure of the mesospheric Na layer can be characterized by the column abundance, centroid height, and RMS layer width. The layer parameters are calculated from different moments of the mesospheric Na layer as described by Gardner et al. (1986). Based on the same data as represented in Fig. 8, the temporal variations of column abundance, centroid height and RMS width of the average nocturnal sodium layer are plotted in Fig. 9a–c. In Fig. 9a, the total Na content is found to vary between 8.6×10^9 and $\sim 5.97 \times 10^9 \text{ atoms cm}^{-2}$ while the average abundance is $\sim 7.35 \times 10^9 \text{ cm}^{-2}$. The percentage of variation from maximum-to-minimum abundance over the complete night observation is $\sim 15\%$. The abundance variations show a decreasing trend from sunset to midnight and again increasing trend from midnight to early morning hours. The variation found to be less in comparison to mid latitude site where Gardner et al. (1986) reported the maximum abundance is about 2.5 times of the minimum abundance values. Here, we found the ratio between the values is ~ 1.5 . Simonich et

al. (1979) also reported an average nocturnal variation by a factor of 2 in the sodium column abundance observed over 23° S . Our lidar measurements at Gadanki site show a steady fall in mean column abundance after sunset and a slow rise towards early hours of the day. In summary, the total Na content decreases during evening and reaches minimum value around midnight and then reaches maximum during early morning hours. Most of the Northern and Southern latitude observations show that a decrease of abundance in the early evening, a minimum around midnight, and an increase after midnight (Gardner et al., 1986; Sandford and Gibson, 1970; Simonich et al., 1979; Clemesha et al., 1982). The observed nighttime variation could be the manifestation of semidiurnal variation in the sodium layer (Gardner et al., 1986). It might be due to the existence of solar-atmospheric tides in the layer (Gardner et al., 1986). It is well known that atmospheric tides play an important role in the mesopause region (Chapman and Lindzen, 1970). A number of studies from a southern sub-tropical station (23° S , 46° W) have reported the presence of 12-h oscillation in the sodium layer (Clemesha et al., 1982, 2002; Batista et al., 1985). Photochemistry in night-time, dynamics or both may be responsible for the observed variations in the total Na content. Variations in the atomic oxygen number density could be the probable cause for such variations in the sodium content. Additionally, dynamics associated with the layer through horizontal transport may also play a role in the observed variations. Batista et al. (1985) concluded that the semi-diurnal oscillations observed in the atmospheric sodium layer at 23° S were mainly induced by atmospheric tides. They were unable to identify any definite chemical effects responsible for such oscillations in the sodium layer. However, States and Gardner (1999) reported from mid-latitudes that the variations observed in the sodium layer are forced by photochemical effects and not by tidal influence. The detailed study of these oscillations, from

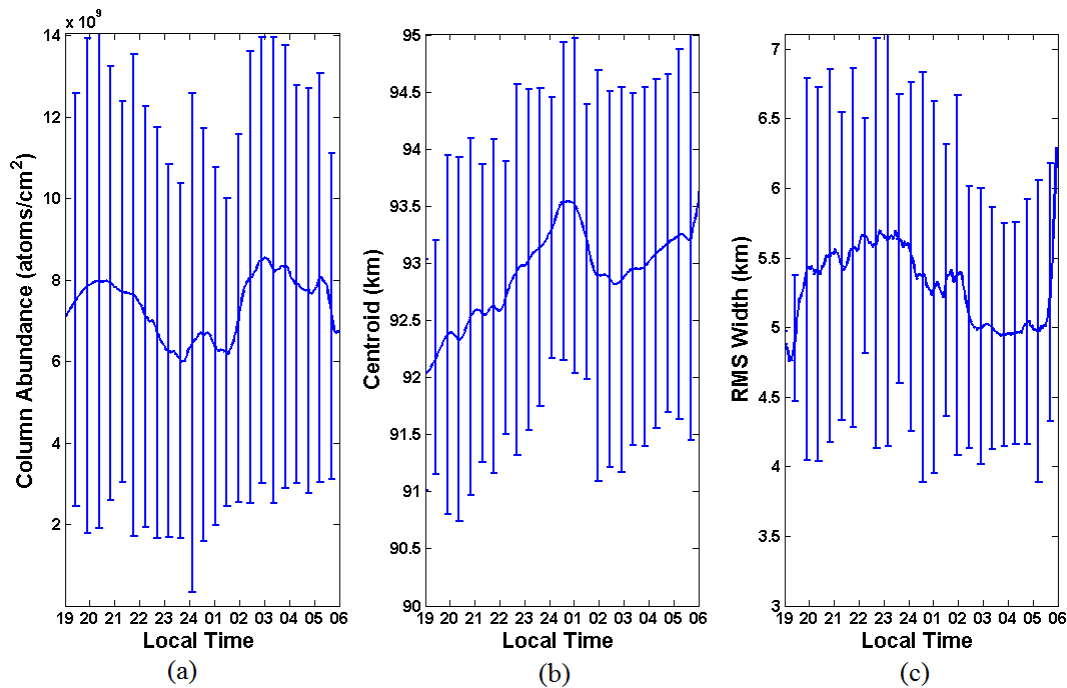


Fig. 9. Mean temporal variations of (a) column abundance, (b) centroid height and (c) RMS width obtained from the year 2005 and 2006.

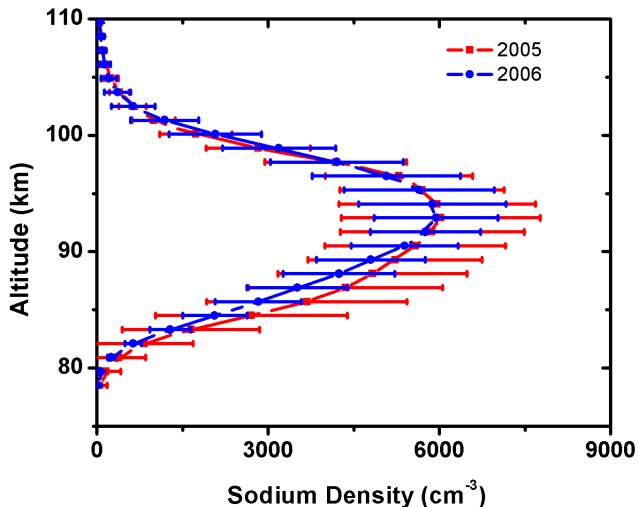


Fig. 10. Annual mean sodium density profiles for the year 2005 and 2006.

the present data is restricted by the fact that sodium measurements with our lidar were obtained only during nighttime, for which the length of data is always less than 11 h.

Figure 9b shows the mean nocturnal variation of the centroid position obtained from January 2005 to December 2006. The nocturnal variation of the sodium layer centroid is a very important parameter to be considered for understanding the layer dynamics (Gardner et al., 1986). The layer

mean centroid position varies from 92 to 93.7 km. The centroid curve shows an increase in the centroid height from early evening to midnight and decreases for an hour and increases again up to early hours. The Gadanki observations are similar to those of Gardner et al. (1986) who reported an increase in centroid height throughout the night with a more pronounced height increase at about 04:00 LST and the average centroid height reported for Urbana data is ~ 92 km.

Figure 9c shows the mean nocturnal variation of RMS width for the same time period as mentioned earlier. The RMS width curve shows an increasing trend from sunset through the middle of the night and then subsequent decrease from midnight to the early morning hours. The mean RMS widths of the layer vary between 4.7 and 6.4 km while the mean RMS width of the layer for the complete data set is 5.3 km and the total width variation is about 1.72 km. Gardner et al. (1986) reported the average RMS width of the layer is 4.5 km with a total width variation of about 600 m. It appears that the layer width is out-of-phase with the centroid height (see Fig. 9b and c).

3.6 Year-to-year variation

Figure 10 shows the mean sodium profiles obtained from the entire measurement period during the year 2005 and 2006. Here, we have discarded September 2005 and October 2005 months due to the observed unexpected larger sodium concentrations. It is evident from the figure that the sodium layer begins to appear from ~ 80 km and it reaches the maximum

values at 93.5 km and 92.9 km during 2005 and 2006, respectively. Further, the density layers decrease closer to zero at ~ 110 km. Statistically, it might be partly due to the total datasets used. Further, it is noted that we had more number of observational days in year 2006 (92 days) compared to the year 2005 (63 days). The observed maximum density (centroid) at 92–93 km is similar to other reported results from different locations (Kirchhoff and Clemesha, 1973; Sandford and Gibson, 1970; Gardner et al., 2005). The annual mean peak layer observed for the two years over Gadanki is at ~ 93 km. It is in good agreement with our earlier result on seasonal variation of centroid height (see Sect. 3.4.2). States and Gardner (1999) observed the peak Na density for the annual mean is 3040 cm^{-3} at 91.8 km and She et al. (2000) observed peak density at 91 km. Gardner et al. (2005) found that the annual mean is $\sim 3700 \text{ cm}^{-3}$ at 90 km over the South Pole. Photo-ionization has been suggested as the loss mechanism which produces steep top-side by removing atoms through upward diffusion processes (Hanson and Donaldson, 1967). However, the mean sodium profile for 2006 shows less variability in comparison to 2005.

It has already been concluded that the Na layer (especially above 90 km) is controlled by ionic rather than neutral chemistry (Plane, 1991). On the bottom side of the layer, the sodium density falls off less rapidly. A rapid decrease in the atomic Na number density on the lower side of the layer is mainly caused by the corresponding decrease in atomic H and O (Clemesha et al., 1995). With respect to the bottom side of the sodium layer, a number of loss mechanisms for the removal of sodium have been suggested in the literature: these include oxidation, mainly by O_2 and O_3 , the formation of cluster ions, and attachment of aerosols particles (Clemesha et al., 1995; Kirchhoff et al., 1981; Plane, 1991; Richter and Sechrist, 1979a; Granier et al., 1985; Hunten, 1981).

4 Summary

For the first time, we have presented the seasonal and nocturnal variation of observed sodium layer parameters based on lidar data collected during two years over Gadanki, India. Our major findings are as follows:

- The sodium lidar data used in this study were collected over 166 nights during the period from January 2005 to December 2006. Often, Gadanki profiles show double-peak structure with primary and secondary at 97 km and 87 km. In most of Gadanki nocturnal observations, it is seen that the peak height decreases throughout the night. Such descending structure represents perturbation due to atmospheric wave motion.
- The seasonal variation of sodium density peaks in September, December and March. The observed maximum during September needs larger database to conclude. The present study had only few number of ob-

servations (2 days). The magnitude of sodium density in December and March is less than the magnitude of sodium density in September. The maximum sodium density occurred in all the months is approximately at a height of 95 km. The seasonal column abundance shows maximum during autumn equinox and minimum in the winter months. The seasonal variation of the centroid height does not reveal any significant variations and the seasonal variation of RMS width value is $\sim 20\%$ more than the low-, mid- and high-latitudes.

- The mean nocturnal column abundance shows that the total Na content decreases during evening and reaches a minimum value around midnight and then reaches a maximum during early morning hours. The observed night-time variation could be the manifestation of semidiurnal variation in the sodium layer. The mean nocturnal centroid height alters between 92 and 93.7 km. The average nocturnal centroid shows an increase in the centroid height from early evening to midnight and decreases for an hour and increases again up to early morning hours. The mean nocturnal RMS width of the layer varies between 4.7 and 6.4 km.
- The annual mean sodium profile for the period of 2005 and 2006 depicts that the sodium layer starts from the height ~ 80 km and it reaches the average value of ~ 93 km for the two years and then the density decreases and close to zero at ~ 110 km.

Acknowledgements. The Laboratoire de l'Atmosphère et des Cyclones (LACy) is supported by the French Centre National de la Recherche Scientifique (CNRS)/Institut National des Sciences de l'Univers (INSU) and the Conseil Régional de la Réunion. One of the authors, P. Vishnu Prasanth, acknowledges the Conseil Régional de la Réunion and the Laboratoire de l'Atmosphère et des Cyclones (LACy) for the financial support under post-doctoral fellowship scheme. The National Atmospheric Research Laboratory (NARL) is operated by Department of Space (DOS), Government of India.

Topical Editor C. Jacobi thanks two anonymous referees for their help in evaluating this paper.



The publication of this article is financed by CNRS-INSU.

References

- Batista, P. P., Clemesha, B. R., Simonich, D. M., and Kirchhoff, V. W. J. H.: Tidal oscillations in the atmospheric sodium layer, *J. Geophys. Res.*, 90, 3881–3888, 1985.
- Beatty, T. J., Collins, R. L., Gardner, C. S., Hostetler, C. A., and Sechrist Jr., C. F.: Simultaneous radar and lidar observations of

- sporadic E and Na layers at Arecibo, *Geophys. Res. Lett.*, 16, 1019–1022, 1989.
- Beatty, T. J., Hostetler, C. A., and Gardner, C. S.: Lidar observations of gravity wave and their spectra near the mesopause and stratopause at Arecibo, *J. Atmos. Sci.*, 49, 477–496, 1992.
- Bhavani Kumar, Y., Sivakumar, V., Rao, P. B., Krishnaiah, M., Mizutani, K., Aoki, T., Yasui, M., and Itabe, T.: Middle atmospheric temperature measurements using ground based instrument at a low latitude, *Ind. J. Rad. Space Phys.*, 29, 249–257, 2000.
- Bhavani Kumar, Y., Narayana Rao, D., Sundara Murthy, M., and Krishnaiah, M.: Resonance lidar system for mesospheric sodium measurements, *Opt. Eng.*, 46(8), 1, doi:10.1117/1.2767271, 2007a.
- Bhavani Kumar, Y., Vishnu Prasanth, P., Narayana Rao, D., Sundaramurthy, M., and Krishnaiah, M.: The first lidar observations of the nighttime sodium layer at low-latitudes, Gadanki (13.5° N, 79.2° E), *Earth Planets Space*, 59, 601–611, 2007b.
- Bowman, M. R., Gibson, A. J., and Sandford, M. C. W.: Atmospheric sodium measurements by a tuned Laser Radar, *Nature*, 221, 456–457, 1969.
- Blamont, J. E., Chanin, M. L., and Megie, G.: Vertical distribution and temperature of the nighttime atmospheric sodium layer obtained by laser backscatter, *Ann. Geophys.*, 28, 833–838, 1972.
- Chamberlain, J. W.: Resonance scattering by atmospheric sodium I. Theory of the intensity plateau in the twilight airglow, *J. Atmos. Terr. Phys.*, 9, 73–89, 1956.
- Chapman, S. and Lindzen, R. S.: *Atmospheric tides*, D. Reidel Press, Dordrecht, Holland, 200 pp, 1970.
- Clemesha, B. R., Kirchhoff, V. W. J. H., Kirchhoff, D. M., Takahashi, H., and Batista, P. P.: Simultaneous observations of sodium density and the NaD, OH(8,3), and OI5577- A^o nightglow emissions, *J. Geophys. Res.*, 84, 6477–6482, 1979.
- Clemesha, B. R., Simonich, D. M., Batista, P. P., and Kirchhoff, V. W. J. H.: The diurnal variation of atmospheric sodium, *J. Geophys. Res.*, 87, 181–186, 1982.
- Clemesha, B. R., Sahai, Y., Simonich, D. M., and Takahashi, H.: Nighttime Na-D Emission observed from a Polar-Orbiting DMSP Satellite – Comment, *J. Geophys. Res.*, 95, 6601–6606, 1990.
- Clemesha, B. R., Simonich, D. M., Takahashi, H., Melo, S. M. L., and Plane, J. M. C.: Experimental evidence for photochemical control of the atmospheric sodium layer, *J. Geophys. Res.*, 100, 18909–18916, 1995.
- Clemesha, B. R., Simonich, D. M., Batista, P. P., and Batista, I. S.: Lidar observation of atmospheric sodium at an equatorial location, *J. Atmos. Terr. Phys.*, 60, 1773–1778, 1998.
- Clemesha, B. R., Batista, P. P., and Simonich, D. M.: simultaneous measurements of meteor winds and sporadic sodium layers in the 80–110 km region, *Adv. Space. Res.*, 27, 1679–1684, 2001.
- Clemesha, B. R., Batista, P. P., and Simonich, D. M.: Tide-induced oscillations in the atmospheric sodium layer, *J. Atmos. Solar Terr. Phys.*, 64, 1321–1325, 2002.
- Clemesha B. R., Simonich, D. M., Batista, P. P., Vondrak, T., and Plane, J. M. C.: Negligible long-term temperature trend in the upper atmosphere at 23° S, *J. Geophys. Res.*, 109, D05302, doi:10.1029/2003JD004243, 2004.
- Collins, R. L., Nomura, A., and Gardner, C. S.: Gravity waves in the upper mesosphere over Antarctica, Lidar observations at the South Pole and Syowa, *J. Geophys. Res.*, 99, 5475–5485, 1994.
- Fan Yi, Zhang Shaodong, Zeng Haijian, He Yujin, Yue Xianchang, Liu Jingbo, Lv Hongfang, and Xiong Donghui: Lidar observations of sporadic Na layers over Wuhan (30.5° N, 114.4° E), *Geophys. Res. Lett.*, 29, 59.1–59.4, 2002.
- Fan, Z. Y., Plane, J. M. C., Gumbel, J., Stegman, J., and Llewellyn, E. J.: Satellite measurements of the global mesospheric sodium layer, *Atmos. Chem. Phys.*, 7, 4107–4115, 2007, <http://www.atmos-chem-phys.net/7/4107/2007/>.
- Fussen, D., Vanhellemont, F., Bingen, C., Kyrola, E., Tamminen, J., Sofieva, V., Hassinen, S., Seppala, A., Verronen, P., Bertaux, J. L., Hauchecorne, A., Dalaudier, F., Renard, J. B., Fraisse, R., d’Andon, O. F., Barrot, G., Mangin, A., Theodore, B., Guirlet, M., Koopman, R., Snoeij, P., and Saavedra, L.: Global measurement of the mesospheric sodium layer by the star occultation instrument GOMOS, *Geophys. Res. Lett.*, 31, L24110, doi:24110.21029/22004GL021618, 2004.
- Gardner, C. S. and Shelton, J. D.: Density response of neutral atmospheric layers to gravity wave perturbations, *J. Geophys. Res.*, 90, 1745–1754, 1985.
- Gardner, C. S. and Voelz, D. G.: Lidar measurements of gravity wave saturation effects in the sodium layer, *Geophys. Res. Lett.*, 12, 765–768, 1985.
- Gardner, C. S. and Voelz, D. G.: Lidar studies of the nighttime sodium layer over Urbana, Illinois 2. Gravity waves, *J. Geophys. Res.*, 92, 4673–4694, 1987.
- Gardner, C. S., Voelz, D. G., Sechrist Jr. C. F., and Segal, A. C.: Lidar studies of the nighttime sodium layer over Urbana, Illinois, 1. Seasonal and nocturnal variations, *J. Geophys. Res.*, 91, 13659–13673, 1986.
- Gardner, C. S., Senft, D. C., and Kwon, K. H.: Lidar observations of a substantial sodium depletion in the summertime Arctic mesosphere, *Nature*, 332, 142–144, 1988.
- Gardner, C. S., Plane, J. M. C., Pan, W., Vondrak, T., Murray, B. J., and Chu, X.: Seasonal variations of the Na and Fe layers at the South Pole and their implications for the chemistry and general circulation of the polar mesosphere, *J. Geophys. Res.*, 110, D10302, doi:10.1029/12004JD005670, 2005.
- Gibson, A. J. and Sandford, M. C. W.: The seasonal variation of the night time sodium layer, *J. Atmos. Terr. Phys.*, 33, 1675–1684, 1971.
- Gibson, A. J. and Sandford, M. C. W.: Daytime laser radar measurements of the atmospheric sodium layer, *Nature*, 239, 509–511, 1972.
- Granier, C., Jegou, J. P., Chanin, M. L., and Megie, G.: General theory of the alkali metals present in the earth’s upper atmosphere, III, Diurnal variations, *Ann. Geophys.*, 3(4), 445–450, 1985.
- Gumbel J., Fan, Z. Y., Waldemarsson, T., Stegman, J., Witt, G., Llewellyn, E. J., She, C.Y., and Plane, J. M. C.: Retrieval of global mesospheric sodium densities from the Odin satellite, *Geophys. Res. Lett.*, 34, L04813, doi:10.1029/2006GL028687, 2007.
- Hanson, W. B. and Donaldson, J. S.: Sodium distribution in the upper atmosphere, *J. Geophys. Res.*, 72, 5513–5514, 1967.
- Hunten, D. M.: A Study of sodium in twilight, I. Theory, *J. Atmos. Terr. Phys.*, 5, 44–56, 1954.
- Hunten, D. M. and Wallace, L.: Rocket measurements of the sodium dayglow, *J. Geophys. Res.*, 72, 69–79, 1967.
- Hunten, D. M.: A meteor-ablation model of the sodium and potas-

- sium layers, *Geophys. Res. Lett.*, 8, 369–372, 1981.
- Jegou, J. P., Granier, C., Chanin, M. L., and Megie, G.: General theory of the alkali metals present in the Earth's upper atmosphere I, Flux model: Chemical and dynamical processes, *Ann. Geophys.*, 3, 163–176, 1985a.
- Jegou, J. P., Granier, C., Chanin, M. L., and Megie, G.: General theory of the alkali metals present in the Earth's upper atmosphere II, Seasonal and meridional variations, *Ann. Geophys.*, 3, 299–312, 1985b.
- Kirchhoff, V. W. J. H.: Atmospheric sodium chemistry and diurnal variations: An update, *Geophys. Res. Lett.*, 10, 721–724, 1983.
- Kirchhoff, V. W. J. H. and Clemesha, B. R.: Atmospheric sodium measurements at 23° S, *J. Atmos. Terr. Phys.*, 35, 1493–1498, 1973.
- Kirchhoff, V. W. J. H. and Clemesha, B. R.: The atmospheric neutral sodium layer, 2. Diurnal variations, *J. Geophys. Res.*, 88, 442–450, 1983.
- Kirchhoff, V. W. J. H. and Takahashi, H.: Sodium clouds in the lower thermosphere, *Planet. Space Sci.*, 32, 831–836, 1984.
- Kirchhoff, V. W. J. H., Clemesha, B. R., and Simonich, D. M.: The atmospheric neutral sodium layer, 1. Recent modeling compared to measurements, *J. Geophys. Res.*, 66, 6892–6898, 1981.
- Krassovsky, V. I.: Internal gravity waves near the mesopause and hydroxyl emission, *Ann. Geophys.*, 33, 347–356, 1977.
- Kumar, K. K. and Jain, A. R.: L band wind profiler observations of convective boundary layer over Gadanki, India (13.5° N, 79.2° E), *Radio Sci.*, 41, RS2004, doi:10.1029/2005RS00329, 2006.
- Kwon, K. H., Senft, D. C., and Gardner, C. S.: Lidar observations of sporadic sodium layers at Mauna Kea Observatory, Hawaii, *J. Geophys. Res.*, 93(20), 14199–14208, 1988.
- Megie, G.: Contribution a l'etude du comportement de l'atmosphere a la mesopause obtenue par sondage laser du sodium, PhD thesis, Univ. Pierre et Marie Curie, Paris, 1976.
- Megie, G. and Blamont, J. E.: Laser sounding of atmospheric sodium interpretation in terms of global atmospheric parameters, *Planet. Space Sci.*, 25, 1093–1109, 1977.
- Newman, A. L.: Nighttime Na D emission observed from a polar-orbiting DMSP satellite, *J. Geophys. Res.*, 93(A5), 4067–4075, doi:10.1029/88JA01123, 1988.
- Plane, J. M. C.: The chemistry of meteoric metals in the Earth's upper atmosphere, *Int. Rev. Phys. Chem.*, 10, 55–106, 1991.
- Plane, J. M. C.: Atmospheric chemistry of meteoric metals, *Chem. Rev.*, 103, 4963–4984, 2003.
- Plane, J. M. C.: A time-resolved model of the mesospheric Na layer: constraints on the meteor input function, *Atmos. Chem. Phys.*, 4, 627–638, 2004, <http://www.atmos-chem-phys.net/4/627/2004/>.
- Plane, J. M. C., Cox, R. M., Qian, J., Pfenninger, W. M., Papen, G. C., Gardner, C. S., and Espy, P. J.: Mesospheric Na layer at extreme high latitudes in summer, *J. Geophys. Res.*, 103(D6), 6381–6389, 1998.
- Plane, J. M. C., Gardner, C. S., Yu, J., She, C. Y., Garcia, R. R., and Pumphrey, H. C.: Mesospheric Na Layer at 40° N: modeling and observations, *J. Geophys. Res.*, 104(D3), 3773–3788, 1999.
- Richter, E. S. and Sechrist Jr., C. F.: A cluster ion chemistry for the mesospheric sodium layer, *J. Atmos. Terr. Phys.*, 41, 579–586, 1979a.
- Richter, E. S. and Sechrist Jr., C. F.: A meteor ablation-cluster ion atmospheric sodium theory, *Geophys. Res. Lett.*, 6, 183–186, 1979b.
- Richter, E. S., Rowlett, J. R., Gardner, C. S., and Sechrist Jr., C. F.: Lidar observation of the mesospheric Na layer over Urbana, Illinois, *J. Atmos. Terr. Phys.*, 43, 327–337, 1981.
- Rodgers, C. D.: Inverse methods for atmospheric sounding: theory and practice, 238 pp., World Scientific, Singapore, 2000.
- Rowlett, J. R., Gardner, C. S., Richter, E. S., and Sechrist Jr., C. F.: Lidar observations of wavelike structure in the atmospheric sodium layer, *Geophys. Res. Lett.*, 5, 683–686, 1978.
- Sandford, M. C. W. and Gibson, A. J.: Laser radar measurements of the atmospheric sodium layer, *J. Atmos. Terr. Phys.*, 32, 1423–1430, 1970.
- She, C. Y., Chen, S., Hu, Z., Sherman, J., Vance, J. D., Vasoli, V., White, M. A., Yu, J., and Kreger, D. A.: Eight-year climatology of nocturnal temperature and sodium density in the mesopause region (80–105 km) over Fort Collins, CO (41° N, 105° W), *Geophys. Res. Lett.*, 27, 3289–3292, 2000.
- Simonich, D. M., Clemesha, B. R., and Kirchhoff, V. W. J. H.: The mesospheric sodium layer at 23° S: Nocturnal and seasonal variations, *J. Geophys. Res.*, 84, 1543–1550, 1979.
- Slipher, V. M.: Emission in the spectrum of the light of the night sky, *Publ. Astron. Soc. Pac.*, 41, 262–263, 1929.
- States, R. J. and Gardner, C. S.: Structure of the mesospheric Na layer at 40° N latitude: seasonal and diurnal variations, *J. Geophys. Res.*, 104, 11783–11798, 1999.
- Swider, W.: Enhanced seasonal variation for chemical rates with inverse temperature dependencies: application to seasonal abundance of mesospheric sodium, *Geophys. Res. Lett.*, 12, 589–592, 1985.
- Sze, J. D., Ko, M. K. W., Swider, W., and Murad, E.: Atmospheric sodium chemistry, I. The altitude region 70–100 km, *Geophys. Res. Lett.*, 9, 1187–1190, 1982.
- Takahashi, H., Sahai, Y., Clemesha, B. R., Batista, P. P., and Teixeira, N. R.: Diurnal and seasonal variations of the OH (8, 3) airglow band and its correlation with OI 5577 Å, *Planet. Space Sci.*, 25, 541–547, 1977.
- Tilgner, C. and von Zahn, U.: Average properties of the sodium density distribution as observed at 69° N latitude in winter, *J. Geophys. Res.*, 93, 8439–8454, 1988.
- Vishnu Prasanth, P., Sridharan, S., Bhavani Kumar, Y., and Narayana Rao, D.: Lidar observations of sporadic Na layers over Gadanki (13.5° N, 79.2° E), *Ann. Geophys.*, 25, 1759–1766, 2007, <http://www.ann-geophys.net/25/1759/2007/>.
- von Zahn, U., von der Gathen, P., and Hansen, G.: Forced release of sodium from upper atmosphere dust particles, *Geophys. Res. Lett.*, 14, 76–79, 1987.
- von Zahn, U., Hansen, G., and Kurzawa, H.: Observations of the sodium layer at high latitudes in summer, *Nature*, 331, 594–596, 1988.